A simplified hybrid model for the electrochemical turning process

Essam Soliman
Production Engg. Dept., Faculty of Engg., University of Alexandria, Alexandria, Egypt, 21544
e_soliman@alex.edu.eg

This work provides a simplified hybrid model for the electrochemical turning process. The model considers the basic techniques for electrochemical machining modeling and simulation. It employs experimental data pertaining to the electrochemical recessing process to simplify modeling and simulation of the process. Experimental data includes parameters of work part profile generated after several machining times. Profile parameters are flat and total widths of the profile and profile depth. Experimental data was fed into the model in the form of empirical formulae to replace complex procedures required to determine current density distribution in the machining zone. Experimental data was used to verify the model within a range of machining conditions. Work part simulated and measured profiles were in good agreement.

تقدم هذه الورقة البحثية نموذجا رياضيا مختلطا ومبسطا لعملية الخراطة الكهروكيميائية. يعتمد بناء النموذج على التقنيات الأساسية لنمذجة ومحاكاة القطع الكهروكيميائى لكنه يستخدم النتائج المعملية المرتبطة بعملية الخنق الكهروكيميائى لتبسيط بناء النموذج الرياضي ومحاكاته. تشمل النتائج المعملية المستخدمة في بناء النموذج عناصر شكل العينة بعد القطع. عناصر الشكل هي العمق والعرض الكلى والعرض المستوى. تم إدماج النتائج المعملية في النموذج الرياضي في صورة معادلات لتحل محل الخطوات الرياضية المركبه والمطلوبة لحساب توزيع شده التيار في منطقة القطع. تم استخدام النتائج المعملية للتأكد من قدرة النموذج المقدم على توقع التغير في شكل العينة أثناء القطع. تبين وجود توافق بين النتائج المعملية ونتائج المحاكاة للنموذج المقدم.

Keywords: Electrochemical turning, Modeling, Simulation

1. Introduction

Electrochemical turning is a well defined machining process. It resembles the conventional turning process; however, the conventional turning tool is replaced with a cathode tool which is separated from the anodic rotating work part by a small gap. An electrolyte is pumped though the gap and a potential is applied across the tool and work part to dissolve work part material. Electrochemical turning has the advantage of machining very hard materials that cannot be machined by conventional turning. Also, electrochemically turned surfaces have no residual stresses or heat affected zone.

Recently, electrochemical turning has gained attention as a finishing process. H. Hocheng et al. [1, 2] conducted an experimental study of electrochemical polishing of cylindrical work parts. They used several form-disc like electrodes and conventional cutting tools. Form-disc electrodes was rotated at different speeds. All electrodes were fed parallel to work part axis at different feedrates. Also, several work part materials were used and each work part was rotated at several speeds. They concluded that thin disc like electrodes produce best surface finish, especially when pulsed current is employed. They, also, pointed out that pulsed current is less effective compared to electrode design in improving surface finish of electrochemically polished work parts.

P.S. Pa [3] investigated, experimentally, the effect of electrode design parameters on the electrochemical finishing quality of end turned work parts. Design parameters included electrode size, curvature of edges and geometry of cross section. Work part finishing quality was measured by the average roughness height. The author, also, studied the effect of several process parameters, such as rotational speed of work part, rotational speed of tool, current density and current rating, on work part surface finish. The author

concluded that rotating partial size electrodes produce best finish and optimum work part rotational speed exits, within the range of used process parameters.

T.A. El-Taweel et al. [4] developed a hybrid electrochemical smoothing and roller burnishing process. They used statistical techniques to analyze the effects of different process parameters on roundness of turned work parts. Process parameters included rotational speed, inter-electrode gap, applied potential and burnishing force. They found that the potential is the most dominating factor. They also found that a combination of wide inter-electrode gap and high burnishing force can significantly reduce roundness error. The afro mentioned research wok focused on electrochemical turning from experimental prospective. No attempt, as far as the author is aware of, has been made to model the process. However, modeling of the electrochemical turning process is still within the general umbrella of electrochemical machining theory and modeling techniques developed by several authors. H. Hocheng et al. [5, 6] provided a 2D model for the development of an eroded opening during the electrochemical boring of holes. They assumed that, at each time during machining, each point on the surface of the work part is eroded due to charges emanating from all points on the tool surface. This implies that current lines are inclined to surface of the tool and that of the work part. It, also, implies that current lines are intersecting. In other words, the authors considered the electrolytic conducting zone, between tool and work part, as one region, filled with charges produced by different potential densities. The potential density is inversely proportional to the square of the distance between a point on the surface of the work part receiving the charge and that of the tool emanating the charge. It determines the amount of material removed at each work part surface point. The authors conducted experiments to verify their model. Model simulations and experimental results were in good agreement regarding hole depth, hole profile and machining current.

D. Zhu et al. [7] analyzed the stray machining in electrochemical hole drilling as a major source of process inaccuracy. They pointed out that the stray current effect is inevitable due to the existence of electric potential between the bottom of the electrode tool and the sides of the drilled hole. They conducted numerical simulations to show stray current lines from work part to tool. Then, they proposed the use of a dual pole electrode, with secondary anode, to alleviate the effect of stray machining. Their experimental work showed that the proposed dual pole tool reduces the taper in the drilled hole, thus, improving the electrochemical hole drilling accuracy.

J. Kozak et al. [8, 9] developed a model for electrochemical machining process. The model is basically a two dimensional one. It considered a general form moving and rotating electrode tool. Work part form variations were obtained via simulated changes in a quasi-envelope due to work part dissolution and electrode movement. Simulation software was very efficient in optimizing machining parameters. H. Hardisty et al. [10] developed a 2-D model for electrochemical machining process. Finite element software was developed and used to calculate electric field density and, consequently, dissolution at each finite element of the work part. The model was verified by comparing its results with those obtained from electrochemical machining theory in one dimensional case. Theoretical and finite element simulation results were in good agreement. M. Purear et al. [11] developed a 3-D finite element model for electrochemical machining based on marker method and boundary element approach. The work part was stationary while the electrode was fed in one direction to machine an indentation in a flat surface. Good results were obtained even with complex work part geometries.

The objective of the present work is to exploit the developed electrochemical machining modeling and simulation techniques to model and simulate the electrochemical turning process. However, experimental data is employed to simplify model structure. Such simplified model will help in predicting process behavior and controlling process parameter on-line within any adaptive control system of the process.

2. Process model

Consider a cylindrical work part with an initial radius R_w and a geometrical axis $\bar{z}$, fig. 1. The work part rotates at a speed of N_w around the axis Z which is shifted from $\bar{z}$ by the eccentricity e. The position of the $\bar{z}$ axis is defined, at any point of time t, by the angle φ which is given from the following equation:

$$\varphi = 2\pi N_w t \quad . \tag{1}$$

The tool is a disc like one with radius R_t and height L_t. The center distance between the tool and the work part is given from the equation:

$$C = \sqrt{C_i^2 + e^2 - 2C_i \cdot e \cdot \cos(\varphi)} \quad . \tag{2}$$

Where C_i is the initial center distance between the tool and the work part, at t = 0 and φ = 0. It is given from the equation:

$$C_i = e + R_w + R_t + g_o \quad . \tag{3}$$

Where g_o is the initial minimum gap between the tool and the work part, at t =0. The gap between the tool and work part is filled with an electrolyte having a conductivity κ, which is assumed constant. The electrolyte flows, in the direction shown in fig. 1-b, through a nozzle having a radius R_z. An electric potential, U, is applied across the tool and work part. The present model assumes the following: Current passing from tool to work part is represented by the current lines shown in fig.1-a. The parallel lines represent a constant current density region with width w_f. The inclined lines represent a variable current density region. The total width through which current passes is w_a. Within the constant current density region, the radius of the work part is uniform. Also, uniform variation in radius will take place during machining. However, within the variable current density region, variable work part radius and non uniform radius variations are expected. This complies with the general characteristics of electrochemical machining where sharp corners cannot be generated.

The theoretical determination of w_f and w_a requires complex electric field calculations using finite element techniques. The objective of the present work is to replace such complex calculations by empirical formulae. This is explained in the following experimental work section.

Now, consider an infinitesimal element on the surface of the work part. The element is at angle β with respect to the center line of the tool and work part. It occupies an infinitesimal angle $\partial\beta$. The material dissolved at each infinitesimal element is due to current line emanating from a corresponding infinitesimal element on the surface of the tool. Such current line is viewed as a channel through which negatively charged particles flow from tool to work part causing ionic reaction and consequently material dissolution at the work part surface.

The current flowing through the channel depends on channel length, channel projected cross sectional area and electrolyte conductivity. The channel length, g_c, is the actual gap between the infinitesimal element on the work part and the corresponding one on the tool. It can be calculated from the following equation:

$$g_c = \sqrt{g_{xy}^2 + g_{xz}^2} \quad . \tag{4}$$

Where, g_{xy} is the projected channel length in the $\overline{XY}$ plane while g_{xz} is the projected channel length in the $\overline{XZ}$ plane. The length g_{xy} can be given from the following equation:

$$g_{xy} = \sqrt{(x_2 - x_1)^2 + (y_2 - y_1)^2} \quad . \tag{5}$$

Where, x_i and y_i are geometrical features that can be determined directly by referring to fig. 1-b. They depend on work part radius, R_w, tool radius, R_t, and channel inclination angle, in the $\overline{XY}$ plane, γ_{xy} and the angle β. The tool radius R_t is constant as no electrolytic reaction takes place at the tool. R_w varies, over time, for each infinitesimal element of the work part due to work part dissolution. The angle β ranges from zero to a maximum value determined by the common tangent to work part and tool in the $\overline{XY}$ plane. The angle γ_{xy} is

selected so that channel resistance has a minimum value. To elaborate on this point, fig. 2 shows the variations in channel length, channel projected area and channel resistance with angle γ_{xy}, for two infinitesimal elements at angles β = 0 and 20°. From fig. 2-a, it can be seen that there is a certain value, for the angle for γ_{xy}, at which channel length has a minimum value. Also, fig. 2-b shows that there is another value γ_{xy} at which maximum area takes place. Channel resistance depends on both channel length and area. Its minimum value takes place at the selected value for angle γ_{xy}, fig. 2-c. Fig. 2-d shows the variation in the selected angle depending on the angle β of the infinitesimal element. From the figure, it can be seen that for each infinitesimal element on the work part there is a corresponding selected angle and consequently one corresponding infinitesimal element on the tool.

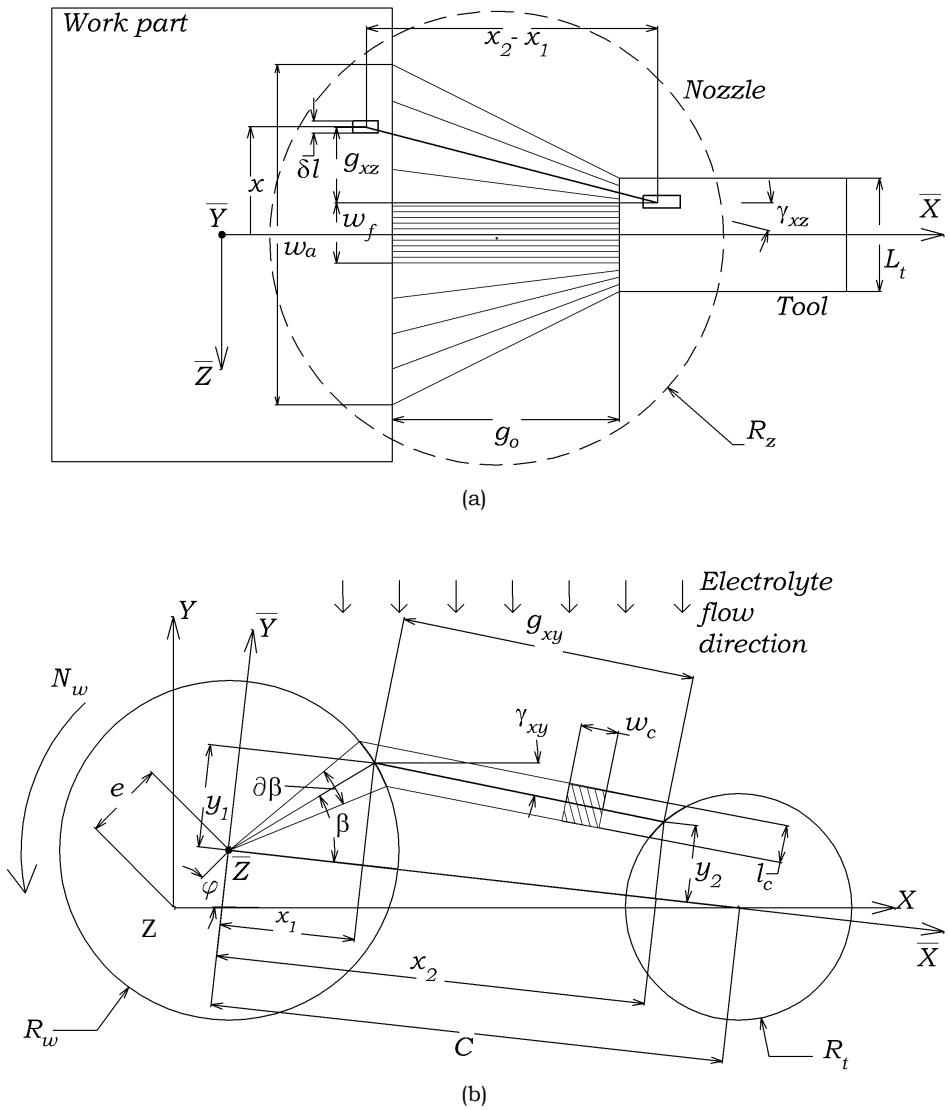

Fig. 1. Schematic of the electrochemical turning process.

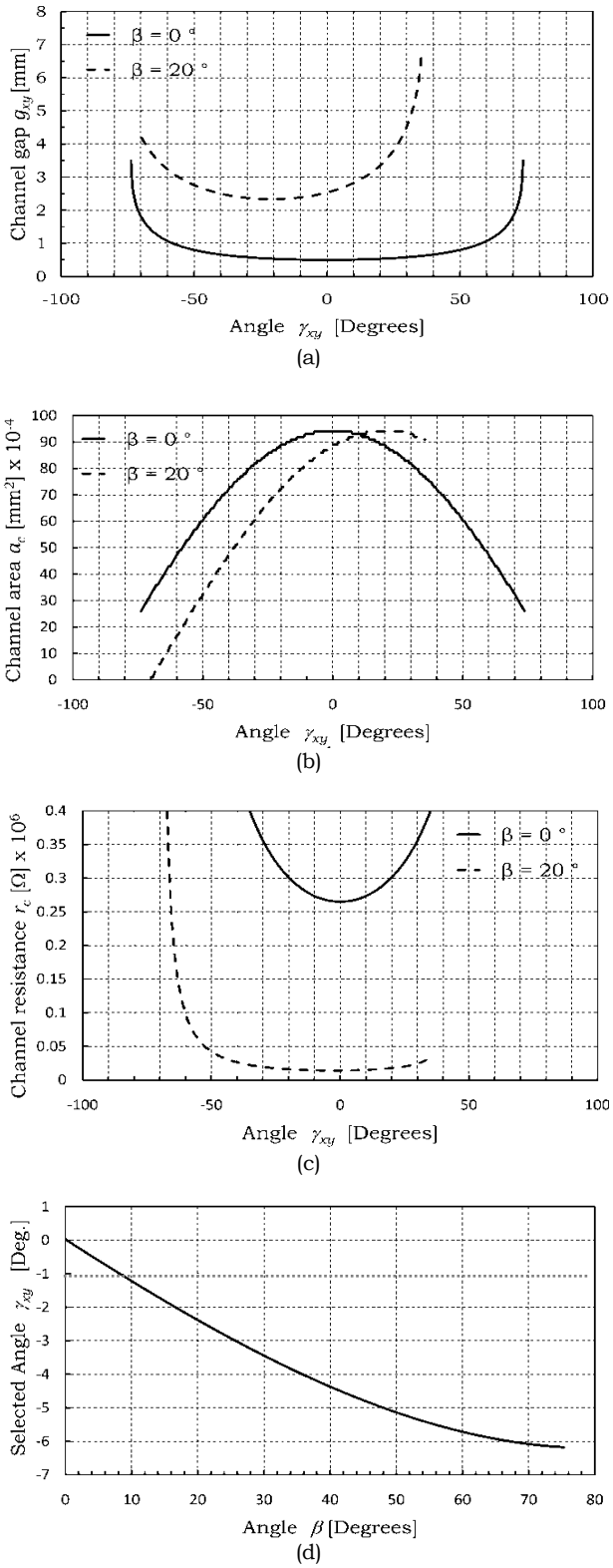

Fig. 2. Variation of selected angle γ_{xy} with work part finite element angle β.

The length g_{xz} depends on the position of the work part infinitesimal element, x, with respect to current lines and can be obtained from the following relation:

$$g_{xz} = \begin{cases} x - \dfrac{w_f}{2} & \Rightarrow x \geq \dfrac{w_f}{2} \\ x = 0 & \Rightarrow x < \dfrac{w_f}{2} \end{cases} . \tag{6}$$

The projected area of the channel, a_c, depends on the selected angel, γ_{xy}, the infinitesimal element angles, β and $\partial\beta$, work part radius, R_w, and the projected gap lengths, g_{xz} and g_{xz}. It can be obtained from the equation:

$$a_c = w_c \cdot l_c \tag{7}$$

Where w_c and l_c can be given from the following equations:

$$w_c = R_w \sin(\partial\beta) \cdot \cos(\beta + \gamma_{xy}), \tag{8}$$

$$l_c = \partial l \left[1 - \left(\frac{g_{xz}}{g_c} \right)^2 \right]. \tag{9}$$

Where, ∂l is the length of the infinitesimal element in the $\overline{X}\overline{Z}$ plan. Channel resistance can then be calculated from the following equation:

$$r_c = \frac{g_c}{\kappa a_c} . \tag{10}$$

The current passing through the channel, I_c, can, then, be determined from the following basic equation:

$$I_c = \frac{U}{r_c} . \tag{11}$$

The amount of material dissolved at the work part infinitesimal element, v_c, can be given according to Faraday's law using the following equations:

$$\upsilon_c = \frac{M \cdot \xi \cdot I_c \cdot \partial t}{F}. \quad (12)$$

Where, ∂t is an incremental time step for model simulation, M is the machining equivalent of work part material, ξ is current efficiency (assumed 100% in the present work) and F is Faraday's constant. Assuming that the work part material dissolves in a radial direction only, υ_c can then be translated into radius variations using the following equation:

$$\partial R_w = \frac{-\upsilon_c}{R_w \cdot \sin(\partial\beta) \cdot \partial l}. \quad (13)$$

The negative sign implies that the work part radius decreases upon machining. Using the above set of equations, the variation in the work part radius, at each work part infinitesimal element, can be determined over time. Consequently, the work part profile can be obtained. However, the widths w_f and w_a, in eq. (6), need to be determined so that the projected channel length g_{xz} can be calculated.

3. Experimental work

An experimental setup that resembles the process model shown in, fig. 1 was assembled on a bench type center lathe. The set up is shown in fig. 3; fig. 3-a is a general view of the set up while fig. 3-b is a zoomed view of the machining zone. The work part is a low carbon steel rod, 1010 (AISI), with 15 [mm] basic diameter and 400 mm length. The work part, held in the three jaws chuck of the lathe, was rotated at 320 RPM.

The tool is a copper disc with 12 [mm] basic diameter and 8 [mm] basic height. The tool is attached to a conducting tool holder which is screwed to a Perspex insulating holder. The Insulating holder moves along a steel frame using a screw-nut mechanism. The steel frame is fixed to the cross slide of the lathe, fig. 3-a. The screw nut mechanism is used to align the axis of the tool and that of the work part in a horizontal plane. The details of the procedure used for setting the tool with respect to the work part are skipped for irrelevancy.

The initial minimum gap, g_o, between tool and work part was set to 0.35 [mm]. NaCl electrolyte, having 200 g/l concentration, was pumped through a 10 [mm] diameter nozzle, through the tube shown in fig. 3-a, to fill the machining gap. The nozzle cap is screwed to the tube so that different nozzles with different shapes and diameters can be used. Electrolyte flow rate was 8 l/min. A direct current potential of 20 V was applied across the machining gap using a homemade direct current power supply that can provide up to 400 A at 7, 14, 20 and 40 V. The –ve terminal of the power supply is connected to the conducting tool holder while its +ve terminal is connected to the work part via lathe bed.

Five cutting tests were conducted for 1, 2, 4, 8 and 16 minutes machining times. The resulting profiles (recesses) were measured using a Carl-Zeiss-Jena universal microscope with scale value 0.001 [mm]. The work part was supported on two V-blocks on the table of the microscope. The axis of the work part was aligned to one measuring direction of the microscope. The diameter of the work part was measured at 0.2 [mm] intervals for each profile. Procedure was repeated for two sections and averaged profiles were calculated. The resulting profiles are shown in fig. 4.

Each profile was identified by three parameters; the first one is the depth of the profile, h, the second one is the width of the flat or uniform machining region, w_f, and the third one is the maximum or total machining width, w_a. Then, correlations between the machining gap, g, w_f and w_a were obtained using a standard regression procedure. The machining gap is basically the sum of the depth of the profile, h, and the initial minimum gap, g_o. The Fitted and experimental data are shown on fig. 5. The obtained empirical relations are as follows:

$$w_a = -8.4409\ g^2 + 23.345\ g + 1.7467\ . \quad (14)$$

$$w_f = 3.9001\ g^2 - 11.552\ g + 10.661. \quad (15)$$

The correlation factors, R^2, for the above empirical eqs. (14 and 15), are 0.981 and 0.9399 respectively, indicating acceptable coherence between experimental and fitted

data. From fig. 5, one can notice that the correlations were based on six points rather than five cutting tests. The extra point it a hypothetical one for which the machining time is zero, profile depth is zero and both total and flat machining widths are equal to tool height, $w_f = w_a = 8$ [mm].

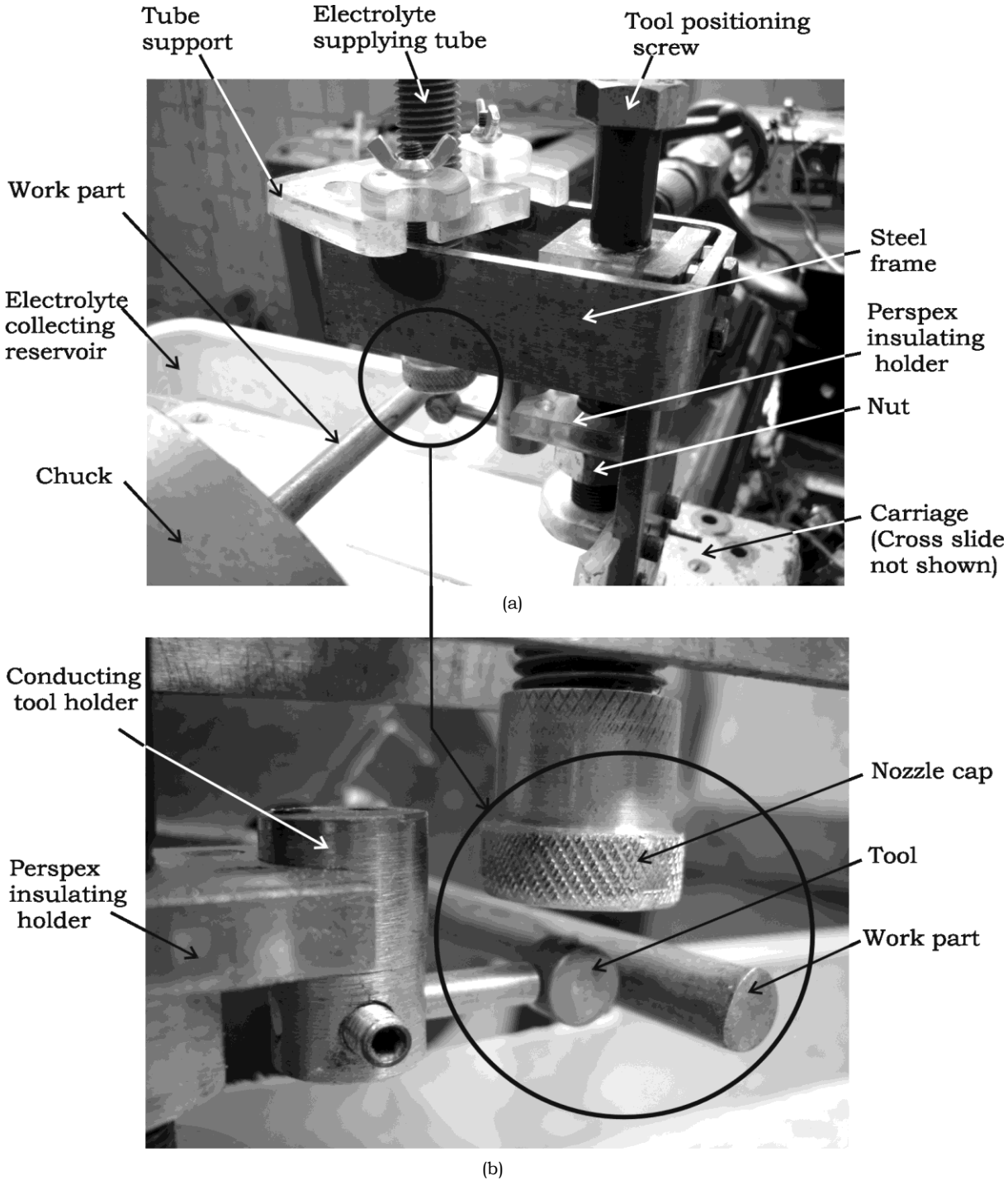

Fig. 3. Experimental setup; a- General view, b- Zoomed view.

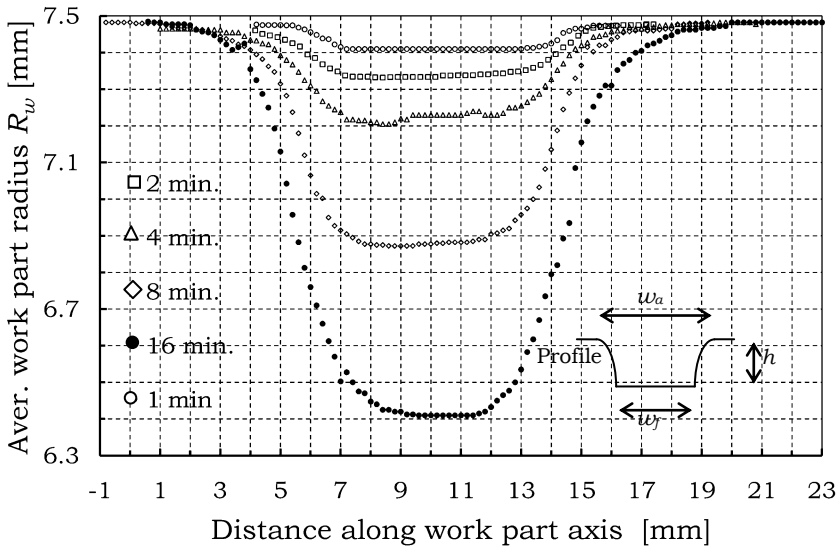

Fig. 4. Experimental profiles of the machined work part.

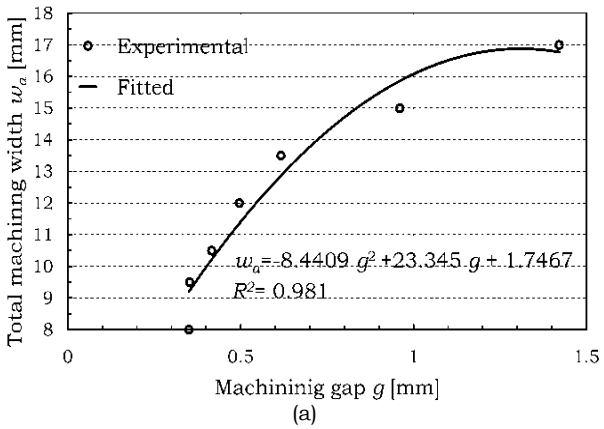

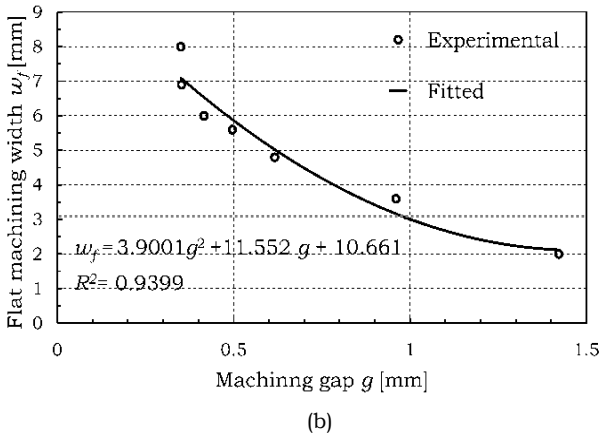

Fig. 5. Experimental correlations of machining gap and; a- total machining width, b- Flat machining width.

4. Model validation results

The correlations of the machining gap, g, w_f and w_a, obtained in the experimental work section were fed into the model. Then work part profiles were simulated for 1, 2 and 4 minutes of machining times. Experimental and simulation results are shown in fig. 6. Experimental and simulation results, for one minute of machining, are shown in fig. 6-a. From the figure, it can be seen that the experimental and simulation results are in good agreement. Fig. 6-b shows similar results for two minutes of machining. Slight deviation between experimental and simulation results can be seen at the upper edges of the profile. This can be attributed to some stray machining from the flat sides of the tool. It is important to mention here that the flat sides of the tool were manually isolated by applying a thin layer of a wax like insulator, normally used for insulating wires of electrical motors. Perhaps imperfection in applying the insulation layer or failure of the layer, due to erosive action of the NaCl electrolyte, resulted in such deviation. However, the depths of the experimental and simulated profiles are almost identical. Fig. 6-c shows the experimental and simulation results for four minutes of machining. Still reasonable agreement between experimental and simulated profiles can be observed.

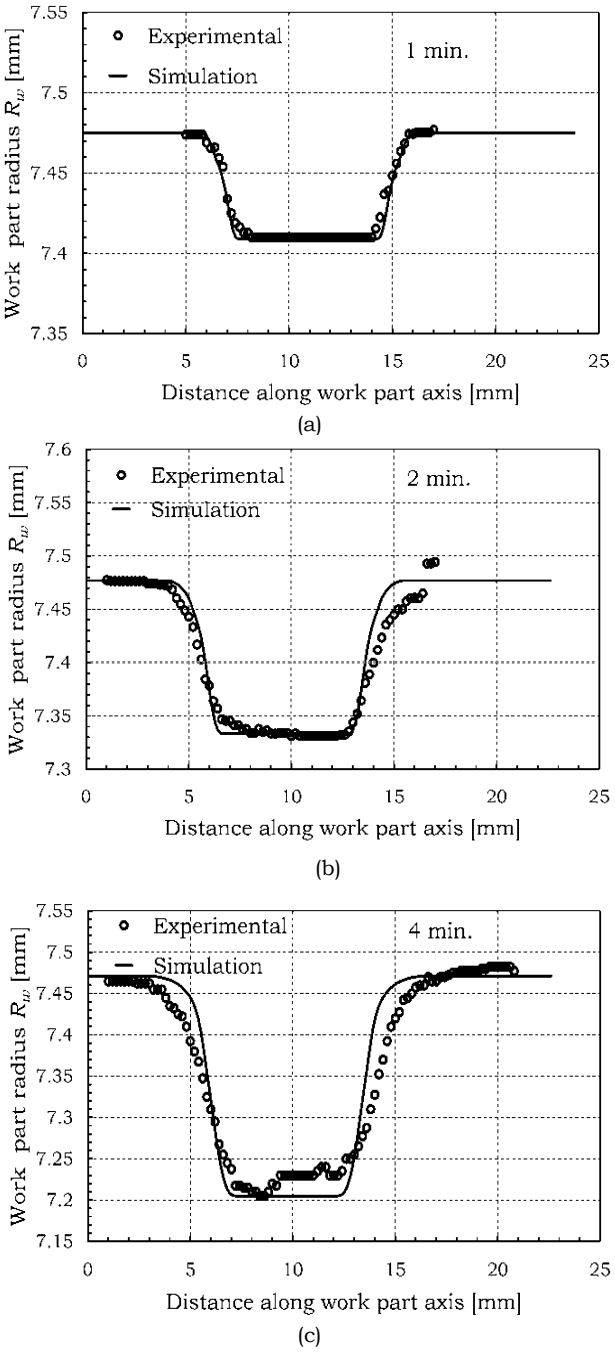

Fig. 6. Experimental and simulated work part profiles.

5. Conclusions

The presented work compiles electrochemical machining theory and experimental data to construct a simplified model for the electrochemical turning process. The model predicts the transient variations in work part profile depth and width upon machining as profile. Experimental work was conducted to support the model and to provide a base for model verification. Simulated and experimental work part profiles were in good agreement within the range of machining conditions used. This suggests using the model for selecting process parameters and for implementing adaptive control systems for the process.

References

[1] H. Hocheng and P.S. Pa, "Electropolishing of Cylindrical Workpiece Using Disc-form Electrodes", Journal of Material Processing Technology, Vol. 142, pp. 203-212 (2003).

[2] H. Hocheng and P.S. Pa, "The Application of a Turning Tool as the Electrode in Electropolishing", Journal of Material Processing Technology, Vol. 120, pp. 6-12 (2002).

[3] P.S. Pa, "Effective Form Design of Electrode in Electrochemical Smoothing of End Turning Surface Finishing", Journal of Material Processing Technology, Vol. 195, pp. 44-52 (2008).

[4] T.A. El-Taweel and S.J. Ebeid, "Improving of Roundness of Cylindrical Parts Using Hybrid Electrochemical Smoothing and Roller Burnishing Process", Proceedings of the 35th International MATADOR Conference, Springer, London, pp. 85-88 (2007).

[5] H. Hocheng, P.S. Pa and S.C. Lin, "Development of Eroded Opening During Electrochemical Boring of Hole", International Journal of Advanced Manufacturing Technology, Vol. 25, pp. 1105-1112 (2005).

[6] H. Hocheng, Y.H. Sun, S.C. Lin and P.S. Kao, "A Material Removal Analysis of Electrochemical Machining Using Flat-End Cathode", Journal of Material Processing Technology, Vol. 140, pp. 264-268 (2003).

[7] D. Zhu and H.Y. Xu, "Improving of Electrochemical Machining Accuracy by Using Dual Pole Tool", Journal of

Material Processing Technology, Vol. 45, pp. 15-18 (2002).

[8] J. Kozak, "Mathematical Models for Computer Simulation of Electrochemical Machining Processes", Journal of Material Processing Technology, Vol. 76, pp. 170-175 (1998).

[9] J. Kozak, A.F. Budzynski and P. Domanowski, "Computer Simulation Electrochemical Shaping (ECM-CNC) Using a Universal Tool Electrode", Journal of Material Processing Technology, Vol. 76, pp. 161-164 (1998).

[10] H. Hardisty, A.R. Mileham and H. Shirvani, "A Finite Element Simulation of the Electrochemical Machining Process", Annals of the CIRP, Vol. 42 (1), pp. 201-207 (1993).

[11] M. Purcar, L. Bortels, B.V. Bossche and J. Deconinck, "3D Electrochemical Machining Computer Simulation", Journal of Material Processing Technology, Vol. 149, pp. 472-478 (2004).

Received April 5, 2008
Accepted May 31, 2008